FMOS: The Fibre Multi-Object Spectrograph VII
Results of PIR engineering run

Masahiko Kimura*[a], Toshinori Maihara[b], Fumihide Iwamuro[b]
Masayuki Akiyama[a], Naoyuki Tamura[a], Naruhisa Takato [a], Kouji Ohta[b], Shigeru Eto[b]
[a]Subaru Telescope, National Astronomical Observatory of Japan, 650 North A'ohoku Pl. Hilo, HI, 96720;
[b]Dept. of Astronomoy, Kyoto University, Kitashirakawa-Oiwakecho, Sakyo-ku, Kyoto,Japan, 606-8502

ABSTRACT

Fibre Multi-Object Spectrograph (FMOS) is the next common-use instrument of Subaru Telescope. FMOS consists of three subsystems; the Prime focus unit for Infrared (PIR), the fibre positioning system/connector units, and the two infrared spectrographs. The PIR was transferred to the Subaru Observatory in the spring of 2005 to check the optical performance on the telescope. As a result of the test observation, we found that the adjustment of the optical axis between PIR and the primary mirror was difficult with the initial design of the corrector alignment stage. Furthermore, the optical axis of the telescope moved over a little owing to an earthquake in Hawaii Island in Oct. 2006. Therefore we decided to modify mechanical structure of PIR, the corrector alignment stage as well as the cable wrapping system. This modification was completed in the summer of 2007. In this proceeding, we report the mechanical structure of the new PIR and the results of the engineering observations.

Keywords: Subaru Telescope, Prime Focus, near Infrared, Spectrograph

1. INTRODUCTION

Fibre Multi-Object Spectrograph (FMOS) is one of the big instruments developed for recent large telescopes, equipping 400 fibres in a 30 arcmin diameter field of the F/2 Prime focus of 8.2m Subaru Telescope[1-13]. The Prime focus unit for Infrared (PIR) was developed in Kyoto University until the spring of 2005[1-3]. After transportation to the summit, we had three engineering observations for optical check of PIR in late 2005. Although the mechanical structure damaged in the last observation run unfortunately, we found that the improvement of the corrector alignment stage is required for the exact adjustment of the optical axis between PIR and the primary mirror. Consequently, we refined the cable wrapping system and the corrector alignment stage with the small shift of the optical axis of the primary mirror caused by the earthquake taking into account. All the subsystem: the modified PIR[1-3], the fibre positioning system (called Echidna) [6-9], the fibre cables with the connectors[12-13], and the two spectrographs (called IRS1, IRS2) [5,10,11], were installed in the telescope at the end of 2007. Various tests for mechanical/optical performance were conducted through engineering observation (Middle/End of December 2007, Jan. and May 2008), in which many stellar images were taken by the sky camera in Echidna to determine the optical aberration of the corrector lenses. In this paper, the mechanical and optical components of modified PIR are described in section 2, and the results of the PIR engineering run are presented in section 3.

2. MECHANICAL STRUCTURE

2.1 PIR: Prime Focus Unit for IR

Subaru Telescope has two prime focus units and three secondary mirrors exchangeable automatically in about five hours in the daytime. One of the two prime focus units is PIR, the front-end unit of the FMOS. PIR consists of seven parts: 1) outer shell structure equipping the instrument rotator and the coupling part with the telescope, 2) corrector movement

*mkimura@subaru.naoj.org;*mkimura@subaru.naoj.org;

Ground-based and Airborne Instrumentation for Astronomy II, edited by Ian S. McLean, Mark M. Casali,
Proc. of SPIE Vol. 7014, 70145K, (2008) · 0277-786X/08/$18 · doi: 10.1117/12.790252

mechanism (CMM) adjusting the center of the corrector lens system to the axis of the primary mirror, 3) focal adjustment mechanism (FAM) focusing Echidna unit on the focal plane of the telescope, 4) Shack-Hartmann camera to measure the accurate optical aberration, 5) Echidna fibre positioner of 400 fibres with the focal plane imager (FPI), 6) operating computer, and 7) cable wrapping system. In the recent engineering observation, we used the sky camera (one of the camera of FPI) to determine the various parameters for the operation of PIR.

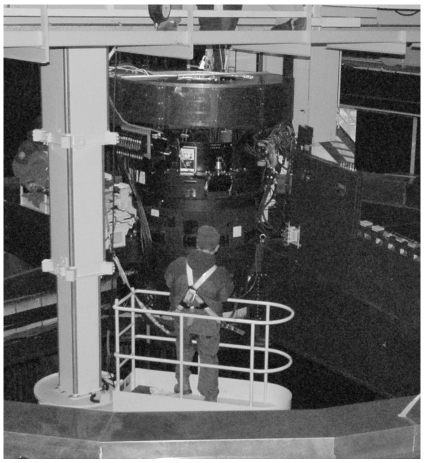

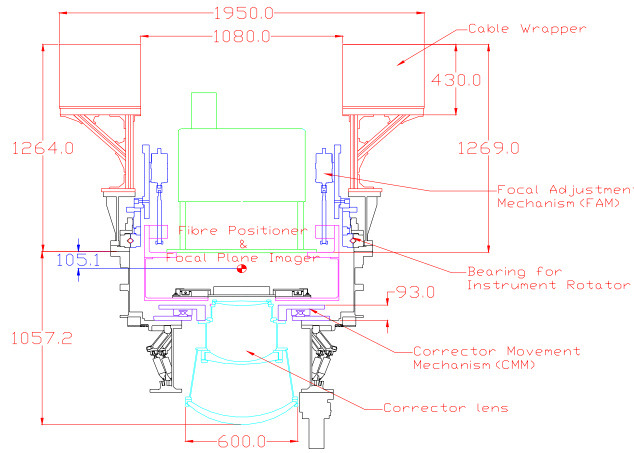

Fig. 1. The Prime focus unit for IR (PIR). Left: Whole view of PIR. Right: Cross section of PIR.

2.2 Corrector Movement Mechanism

The corrector system of three lenses optimized in the near infrared wavelength range has a capability to give images over its 30 arcmin diameter field. The optical aberration of this corrector system is less than 15µm in FWHM, small enough compared with the fibre core diameter of 100µm (equivalent to 1.24 arcsec). In the initial test observation of PIR carried out in 2005, it was difficult to adjust of optical axis using stellar images only by the one direction drive[3]. On the other hand, newly developed adjustment mechanism has two drive axes enable to adjust the optical axis not only along the deforming (elevation, EL) direction of the truss structure of the telescope but also along the horizontal (azimuth, Az) direction. This XY-adjust mechanism has a unique structure; Y-direction movement is supported by the upper plate on the liner guides fixed to the base plate, while X-direction is by the inner bottom plate hanging from the upper plate through the other pair of liner guides. Therefore, the height of this stage is almost the same as that of the previous one axis stage in spite of the capability of two axis drives.

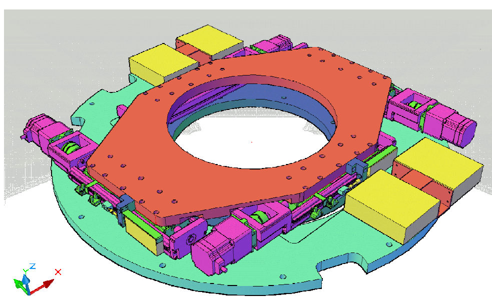

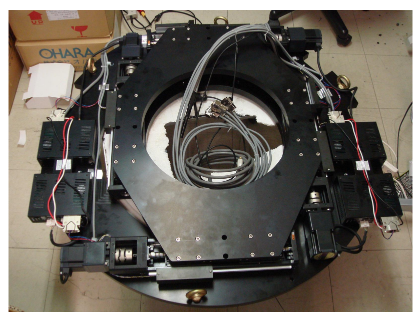

Fig. 2. Whole view of the Corrector Movement Mechanism. The amount of the movement of both axes is ±5mm.

Travel Distance	±5mm @ X,Y-direction
Accuracy	<10µm (flexure < 6 µm)
Height	93mm

Weight	120kg

Table 1. specification for CMM

2.3 Shack-Hartmann system

Shack-Hartmann system is one of the devices for evaluation of the optical performance of the telescope including the corrector lenses. The wave front error is measured with a 16*16 micro lens array in the camera optics. The wave front error is expanded in a series of Zernike's coefficient by the mirror analysis software of the Subaru telescope; enable us to determine the best XY position of CMM as a function of the telescope EL angle. Coma aberration (A31 and A3-1) is sensitive to the XY position of CMM, while defocus (A20) corresponds to the position of FAM stage.

2.4 Cable wrapper for PIR

The PIR has an instrument rotator to compensate the intrinsic field rotation of the Alt-Az mount type telescope. Since many cables such as power cables, signal cables and coolant tubes are necessary for the inner instruments, we have to connect them without restriction of smooth rotation of the instrument rotator. Such a device is called a cable wrapping system. Although there are many products distributed in commerce for industrial machines, these cable wrappers are designed for use on a stable floor. On the other hand, the cable wrapper of PIR should work by almost constant torque at any inclination angle to keep the observational performance of the system independent of a pointing direction of the telescope. In addition, we had the endurance test of the CW/CCW rotation of over 100 times round-trip at EL=14 deg. The torque fluctuation at various EL angles was also measured.

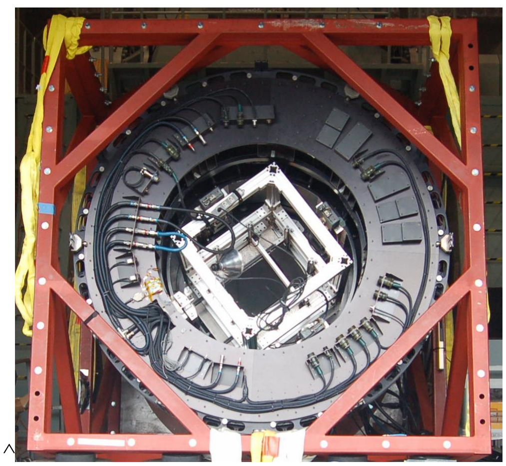

Fig. 3. Top view of Cable wrapper. This photo is taken during the tilting test. Normally, a top cover is attached to the top of the cable wrapper.

Rotation angle during Observation	±180deg @ CW,CCW-direction
Rotation angle of mechanical range	±200deg @ CW,CCW-direction
Max speed of Rotation	1.5 deg/sec
Indemnity EL angle	35 ~ 89 deg
Accessible EL angle	15 ~ 89 deg
Outer Diameter	Φ 1950 mm
Inner Diameter	Φ 1080 mm
Height	430 mm
Weight	350 kg without cables

Table 2. specification for Cable wrapper

The cable wrapper is connected with the instrument rotator via an driving arm, rotating the wrapper within ±180 deg. A torque sensor with a strain gauge is installed in the base of this arm to measure the driving torque by sampling the output voltage value.

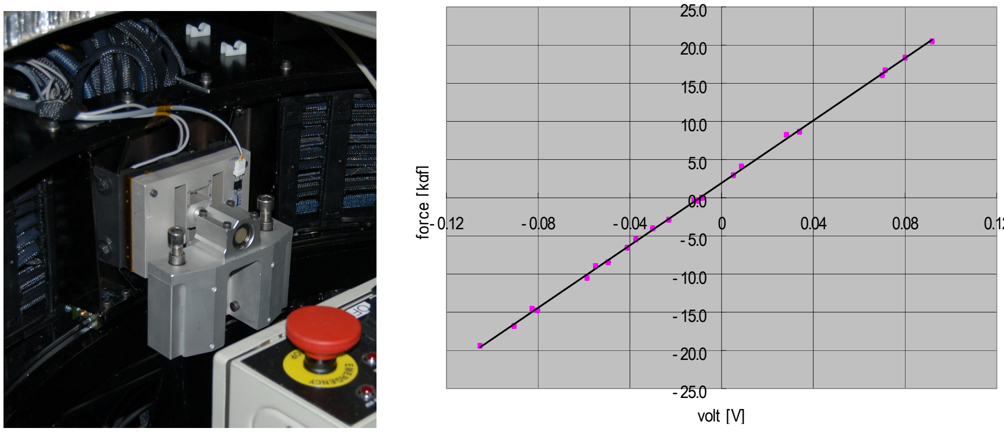

Fig. 4. Left: View of the torque sensor. Right: Relation of output voltage[v] and force [kgf].Output voltage is measured by an AD board in the operating computer. The relation between the voltage and the force is calibrated by a spring scale:

$$\text{Force [kgf]} = 204.4 * \text{volt [V]} + 1.933$$

2.5 Focal Plane Imager for Fibre Positioner

The focal plane imager (called FPI) has two cameras: one is the sky camera for taking a sky image, the other is the spine camera for taking the position of all the spine tips. The sky camera checks the direction of the telescope referring the position of a number of bright stars with R-band (700nm) filter. Both cameras cover the whole area of the focal plane in conjunction with a XY-stage. The actual performance of Echidna is described in Akiyama et al.[14] in detail.

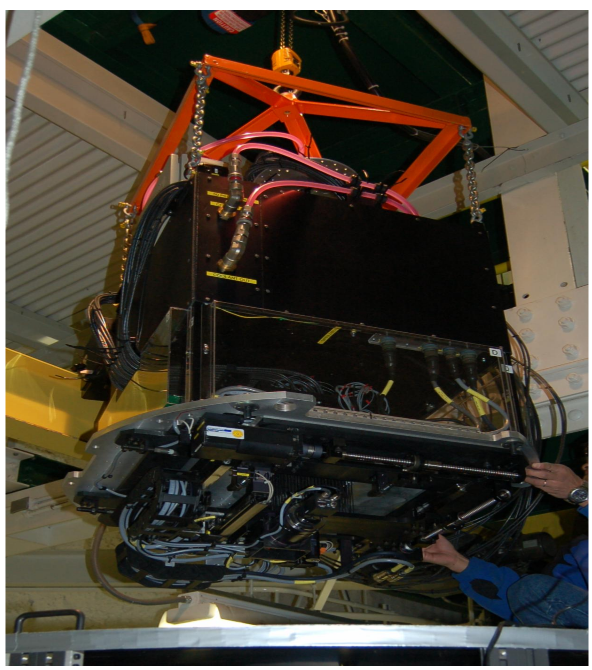

Fig. 5. Whole view of Echidna

3. RESULTS

3.1 Cable Wrapper

We measured the torque fluctuation during rotation of the new cable wrapper using the torque sensor attached to the base of the driving arm. The results show that the torque is almost constant value of 7-9 kgfm at any angle of instrument rotator under any inclination condition. There is no significant differences of the fluctuation profile between before and after the endurance test of 100 times CW/CCW round-trip at EL=14 deg. The torque fluctuation profile shows a stable small hysteresis behavior in the CW/CCW round-trip of the instrument rotator, because of the non-symmetric inner structure of the cable wrapper. Fig6 shows the results of the torque measurement at EL=14 deg.

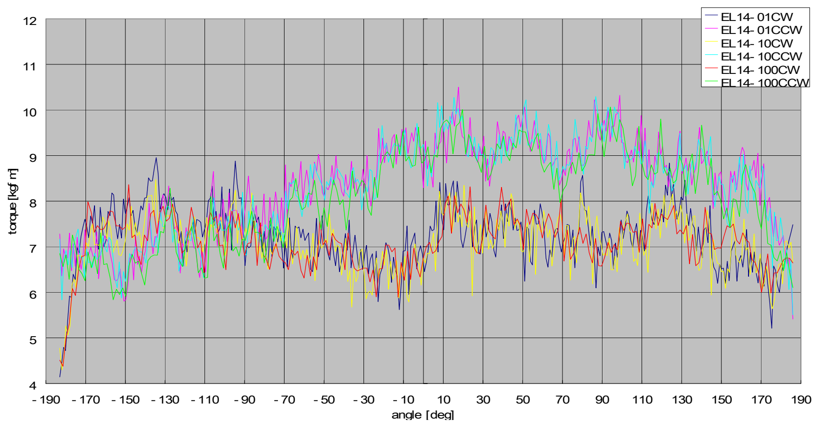

Fig. 6. Torque fluctuation profile during endurance test. The profile measured at first time, after 10 times, and after 100 times round-trip at EL=14 deg are plotted.

	CW direction		CCW direction	
	Average of torque value [kgf m]	Dispersion of torque value [kgf m]	Average of torque value [kgf m]	Dispersion of torque value [kgf m]
EL90	5.48	0.63	6.59	0.55
EL45	8.22	0.57	7.47	0.95
EL14	8.57	0.65	8.40	0.98

Table3. summary of the measured vale of torque.

3.2 Optical Alignment

The center of the corrector lens system is aligned to the optical axis of the primary mirror minimizing the Coma aberration of the stellar image, which is evaluated as a wave front error expanded in a series of Zernike's coefficient. Thus the wave front error determined by the Shack-Hartmann system for each CMM-XY positions indicates the best position as a function of telescope EL angle. Fig.7 shows the Zernike's coefficients corresponding to Coma aberrations (A31 and A3-1) and Defocus (A20) calculated by the Subaru mirror analysis software. We found that the best position of CMM is (X,Y)=(3.7,-3.4) almost independent of the EL angle of the telescope. The position of the optical axis of the telescope based on the FPI coordinate is measured as a distortion center of the field described in the following subsection.

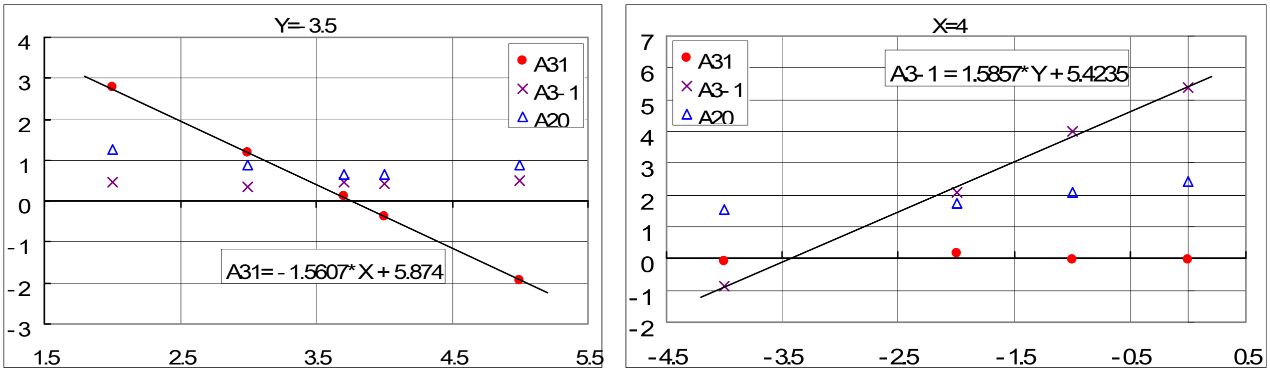

Fig. 7. Zernike's constant (A31, A3-1) corresponding to Coma aberration as a function of CMM movement.

Left: moved along X-axis, fixed Y=-3.5, Right: moved along Y-axis, fixed X=4.0

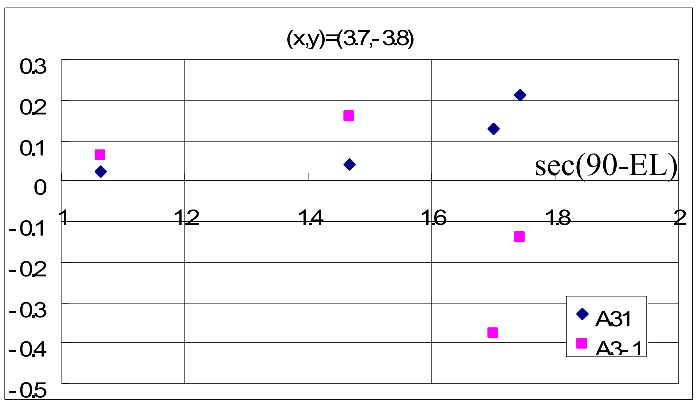

Fig. 8. Zernike's constant (A31, A3-1) as a function of sec(EL angle) with a fixed value of (X,Y)=(3.7,-3.8).

No significant change was detected at elevation higher than 40 deg. (sec(90-EL)<1.47)

3.3 Optical Measurement

We observed the field including an open cluster (M38; 05:28:42, +35:49:48) with tiling the sky camera to determine the direction of the x, y axes of the sky camera (or FPI) coordinate, the pixel scale, and the distortion map of the field. The images were taken with four tiling patterns of about hundred exposures, respectively. We used latter three maps to determine the above parameters: 11 *11 exposures at central region (MAP2), 3*31 exposures along north-south direction (MAP3), and 31*3 exposures along east-west direction (MAP4).

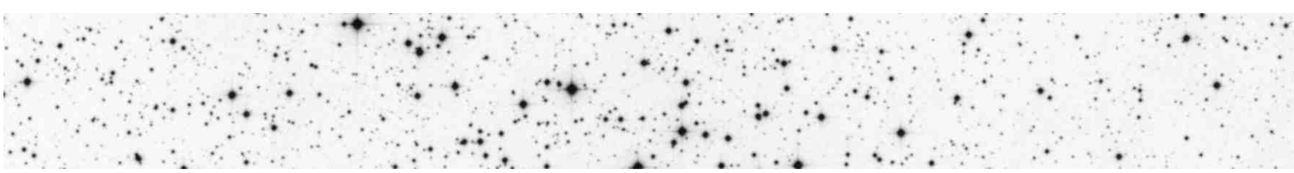

Fig. 9. Combined image of M38 corresponding 31*3 field of view of the sky camera (MAP4).

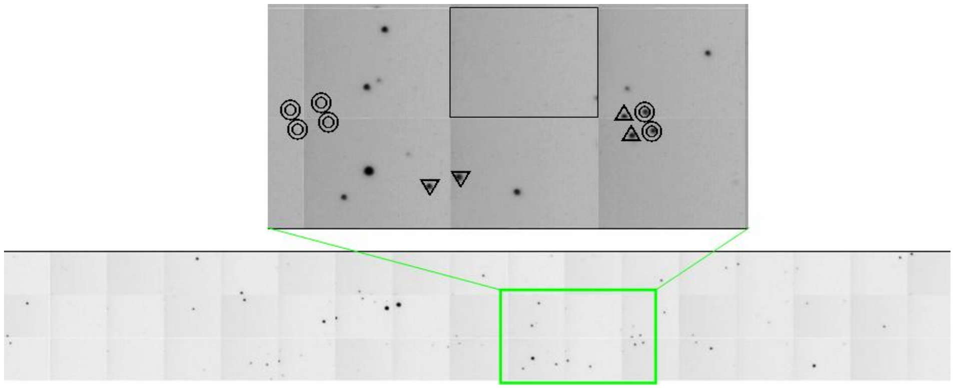

Fig.10. Tiling images of sky camera at M38 (central region of MAP4 shown in Fig.9). Circle, triangle and inverted triangle are same objects. The rectangle of upper view is corresponds to an one shot image for sky camera (1.3 arcmin by 1.0 arcmin field of view)

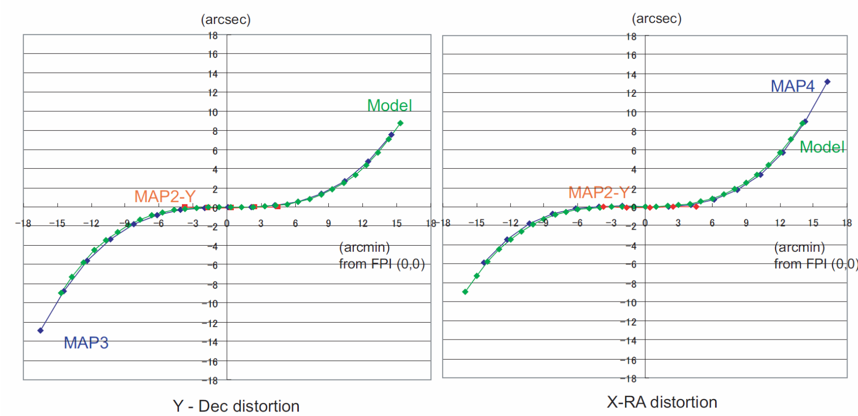

Fig.11. The measured distortion of the corrector lens. Horizontal axis is the distance from the center of FPI (0,0) in arcmin. Vertical axis is the offset from the position without distortion converted with the scale of 0.0124 arcsec/µm. Left) in Y (or Dec) direction, MAP2-Y and MAP3 results are shown, respectively with the ray trace model over-plotted. The model is offset by −1.0 arcmin to match the observed distortion curve. Right) in X (or RA) direction, MAP2-X and MAP4 results are shown. The model is offset by +0.3 arcmin.

The field of view of the sky camera is 1.3’×1.0’, and the pixel scale of the sky camera is 0.10”/pixel.

The measured distortion center (or optical axis of the telescope including the corrector lenses) of +0.3,-1.0 arcmin in RA, DEC in the FPI coordinate is separated from the center of the instrument rotator of +1.7, -1.5 arcmin. The above observation was carried out with the real rotator angle around 0 deg. Here, the center of the instrument rotator is fixed relative to FPI coordinate, while the distortion center travel around the center of the instrument rotator with a diameter of 4.3 arcmin, because the axis of the instrument rotator is located at different position from the optical axis of the telescope. Since this position difference cannot be fixed (PIR does not have a hexapod mount), we have to operate Echidna to compensate the position shift by “tweaking” fibres in the outer field between long exposures.

4. CONCLUTIONS

We have developed the next common-use instrument of Subaru telescope, FMOS, for about ten years. After all the subsystem was installed in the telescope at the end of 2007, various tests and engineering observations were carried out in Dec.2007, Jan. and May 2008.

1) We developed the flat stage for the XY-adjustment mechanism of the corrector lens. This mechanism enables us to align the center of the corrector lenses to the optical axis of the primary mirror.

2) The new cable wrapper was also developed. The endurance test of the CW/CCW round-trip at EL=14deg shows that the driving torque is almost constant values of 7-9 kgfm throughout the movement range of instrument rotator, and at any EL angle.

3) We determined that the best position of CMM (X,Y) is (3.7,-3.4) to minimize the Coma aberration from the results of Shack-Hartmann measurement.

4) From the tiling images of the sky camera, we found that the field of view of the sky camera is 1.3'×1.0' with a pixel scale of 0.10"/pixel. The distortion is about 8" at the edge of the field.

5) The optical performance of the telescope including the corrector lens system is 0.3-0.5" from the series of Zernike's coefficient measured by the Shack-Hartmann system. The actual image size (incl. seeing) is 0.6-0.8" under typical seeing condition.

ACKNOWLEDGEMENT

FMOS project is managed and operated by the National Astronomical Observatory of Japan. The authors wish to thank Day crew members and Software member for valuable discussion and continuous support of this work.

REFERENCES

[1] Maihara, T., Ohta, K., Tamura, N., Ohtani, H., and et al., M. A., "Fiber multi-object spectrograph (fmos) for the subaru telescope," in [*Optical and IR instrumentation and detectors*], Iye, M. and Moorwood, A.,eds., *Proc. SPIE* **4008**, 1111–1118 (2000).

[2] Kimura, M., Maihara, T., Ohta, K., and et al., F. I., "Fibre-multi-object spectrograph (fmos) for subaru telescope," in [*Instrument Design and Performance for Optical/Infrared Ground-based Telescopes*], Iye, M.and Moorwood, A., eds., *Proc. SPIE* **4841**, 974–984 (2003).

[3] Kimura, M., Maihara, T., Iwamuro, F., Eto, S., and et al., M. A., "Fmos: The fiber multi-object spectrograph v results of early pir engineering run," in [*Ground-based and Airborne Instrumentation for Astronomy*], McLean, I. and Iye, M., eds., *Proc. SPIE* **6269**, 132 (2006).

[4] Eto, S., Maihara, T., and et al., K. O., "The fiber multi-object spectrograph (fmos) for the subaru telescope iii," in [*Ground-based Instrumentation for Astronomy*], Moorwood, A. and Iye, M., eds., *Proc. SPIE* **5492**, 1314–1318 (2004).

[5] Iwamuro, F., Maihara, T., Ohta, K., Eto, S., Sakai, M., and et al., M. A., "Fmos - the fiber multiple-object spectrograph iv: current status of ohs-based spectrograph," in [*Ground-based and Airborne Instrumentation for Astronomy*], McLean, I. and Iye, M., eds., *Proc. SPIE* **6269**, 431 (2006).

[6] Gilligham, P., Miziarsky, S., Akiyama, M., and V.Klocke, "Echidna - a multi-fiber positioner for the Subaru telescope," in [*Optical and IR instrumentation and detectors*], Iye, M. and Moorwood, A., eds., *Proc. SPIE* **4008**, 1395–1403 (2000).

[7] Moore, A., Gillingham, P., Griesbach, J., and Akiyama, M., "Spine development for the echidna fiber positioner," in [*Instrument Design and Performance for Optical/Infrared Ground-based Telescopes*], Iye, M. and Moorwood, A., eds., *Proc. SPIE* **4841**, 14290-1439 (2003).

[8] Gilligham, P., Moore, A., and et al., M. A., "The fibre multi-object spectrograph (fmos) project: the angloaustralian observatory role," in [*Instrument Design and Performance for Optical/Infrared Ground-based Telescopes*], Iye, M. and Moorwood, A., eds., *Proc. SPIE* **4841**, 985–996 (2003).

[9] Brzeski, J., Gillingham, P., and et al., D. C., "Echidna - the engineering challenges," in [*Ground-based Instrumentation for Astronomy*], Moorwood, A. and Iye, M., eds., *Proc. SPIE* **5492**, 1228–1242 (2004).

[10] Lewis, I., Dalton, G., and et al., A. H., "Developments on the uk fmos project for the subaru telescope," in [*Instrument Design and Performance for Optical/Infrared Ground-based Telescopes*], Iye, M. and Moorwood, A., eds., *Proc. SPIE* **4841**, 1108–1114 (2003).

[11] Dalton, G., Lewis, I., and et al., D. B., "The uk fmos spectrograph," in [*Ground-based and Airborne Instrumentation for Astronomy*], McLean, I. and Iye, M., eds., *Proc. SPIE* **6269**, 136 (2006).

[12] Murry, G., Woodhouse, G., and et al., T. F., "An ultraprecision fiber connector for fmos," in [*iber-based Component Fabrication, Testing, and Connectorization*], Pruneri, V., Dahlgren, R., and Gregory, M., eds., *Proc. SPIE* **4943**, 184–194 (2003).
[13] Murry, G., Luke, P., Robertson, D., and Tamura, N., "A connectorized fiber downlink for fmos," *Proc. SPIE* **5492**, 1383–1394 (2004).
[14] Akiyama, M., Smedley, S., Gillingham, P., Brzeski, J., Farrell, T., Kimura, M., Muller, R., Tamura, N., Takato, N., "Performance of Echidna Fibre Positioner for FMOS on Subaru", 2008, *Proc. SPIE* (in press)